MACHINE LEARNING FOR STABILITY ANALYSIS OF MILLING PROCESS

A Thesis Presented for the

Master of Science

Degree

The University of Tennessee, Knoxville

Kaitlyn C. Daniels

August 2024

Copyright © 2024 by Kaitlyn C. “Katy” Daniels

All rights reserved.

ACKNOWLEDGEMENTS

This project is dedicated to my support system Bridget and Chris Daniels, my parents, who might not have understood what I was talking about, but nonetheless let me talk through the problems I encountered within this thesis, and Andy, my dog, who constantly reminded me to take much-needed breaks like the good boy he is. I also am grateful to acknowledge Juliana Broussard for helping to tutor me in Python, so that this project could come to fruition in a timely manner. I want to thank Dr. Gary Null and Dr. Tony Schmitz for being on my committee. Lastly, I thank Dr. Anahita Khojandi for being my committee advisor and for always believing in me even when I did not believe in myself.

ABSTRACT

The properties related to chatter and the stability of manufacturing milling machines are dependent primarily on parameters such as axial depth of cut, rotary speed rpm, and cutting force. These parameters are used to calculate the milling process and avoid certain cuts that would result in unstable milling. Using applied data science tools for statistical analysis and machine learning models like SHapley Additive exPlanations (SHAP), this research will produce valuable insight into two stability testing methods used in milling machining operations. By leveraging the data, a partitioning model can be used with known stable and unstable points under certain conditions to sort and select the best point(s) to be used in testing on the stability lobe diagram. The aim is to compare the two testing methods of combination and sequencing testing for cost-effectiveness and accuracy in identifying the milling machine's stability boundary which in turn will help with reducing the amount of chatter present in the milling. Recognizing the testing method with the better accuracy will help determine the best sequence of testing and the stopping criteria.

Keywords — Milling, Chatter, Stability Mapping, Partitioning Models, Sequencing, Combination

TABLE OF CONTENTS

Chapter 1

Introduction and General Information..... 1

Background..... 1

Literature..... 1

Goals..... 2

Data Gaps..... 3

Chapter 2

Literature Review..... 4

Previous Research..... 4

Chapter 3

Materials and Methods..... 6

Data Collection..... 6

Stability Limit Matrix..... 6

Stability Map..... 6

Sequencing..... 7

Combination..... 8

Parameters..... 9

Equations..... 9

Equation (1)..... 9

Equation (2)..... 9

Equation (3)..... 10

Equation (4)..... 10

Equation (5)..... 10
Data Analysis Techniques..... 10
Chapter 4
Results and Discussion..... 12
Data Results..... 12
1st Best Point Sequence Output..... 12
2nd Best Point Sequence Output..... 13
3rd Best Point Sequence Output..... 13
4th Best Point Sequence Output..... 13
24C1 Output..... 14
24C2 Output..... 14
24C3 Output..... 14
24C4 Output..... 15
Analysis of Results..... 16
1st Best Point Sequence Output..... 18
2nd Best Point Sequence Output..... 18
3rd Best Point Sequence Output..... 18
24C1 Output..... 18
24C2 Output..... 18
24C3 Output..... 18
SHAP Output..... 18
Chapter 5
Conclusions and Recommendations..... 20

References.....21

Appendix.....23

Vita.....42

LIST OF FIGURES

Figure 1. Simplified Stability Limit Matrix showing 10 lines out of the 10,000..... 23

Figure 2. Stability Limit Matrix of Entire 10,000 Lines.....24

Figure 3. Stability Table with Labeled Rows.....25

Figure 4. Ground Truths with Stability Labeled.....26

Figure 5. RPM Ranges Labeled True (Stable) & False (Unstable) at Specific Axial Depths..... 27

Figure 6. Count of RPM Ranges Labeled True (Rows At or Above Count) & False (Rows Below Count) at Specific Axial Depths With Percentage of Unstable Rows.....28

Figure 7. List of Unstable Row Sets Used for Determining Sequencing's First Best Point 29

Figure 8. Sequencing's First Best Point Selection With Performance Percentages.....30

Figure 9. List of Unstable Row Sets Remaining Used for Determining Sequencing's Second Next Best Point..... 31

Figure 10. Sequencing's Second Next Best Point Selection With Performance Percentages..... 32

Figure 11. List of Unstable Row Sets Remaining Used for Determining Sequencing's Third Next Best Point..... 33

Figure 12. Sequencing's Third Next Best Point Selection With Performance Percentages 34

Figure 13. Empty List of Unstable Row Sets Remaining for Sequencing's Fourth Next Best Point & Displaying Stopping Criteria Reached.....35

Figure 14. Sequencing's Fourth Next Best Point Selection With Performance Percentages

& Displaying Stopping Criteria Reached..... 36

Figure 15. Sequence of Best Point Selections Based on Performance Percentages..... 36

Figure 16. 24C1 Top Best Point Selection With Performance Percentages..... 37

Figure 17. 24C2 Best Points Selection With Performance Percentages..... 38

Figure 18. 24C3 Best Points Selection With Performance Percentages..... 39

Figure 19. 24C4 Best Points Selection With Performance Percentages..... 39

Figure 20. 24C5 Best Points Selection With Performance Percentages..... 40

Figure 21. 24C6 Best Points Selection With Performance Percentages..... 40

Figure 22. Excel Spreadsheet Showing Each Point's MRR and Cost Per Test..... 41

Figure 23. SHAP Analysis Summary Plot Output..... 41

Chapter 1

Introduction and General Information

Background

The milling manufacturing process is a subtractive manufacturing process where a drilling tool removes material via a shearing method from a section of raw material. The process is used in many manufacturing industries for everyday products from golf clubs to industrial products like machine parts. Metal milling can exceed the stable parameters of the tools and materials, so research seeks to optimize the process to make it more economical, reliable, maintainable, and sustainable. Inadequate milling station parameters will result in poor stability which creates undesirable vibrations or resonances that occur between the cutting tool and workpiece called chatter. Chatter can often be heard as an audible noise, will leave irregular and undesirable tool marks on the machined surface, and can occasionally break the tool piece or even damage the machine.

Literature

There are numerous aspects of the milling process that studies have aimed to optimize. Previous research has sought to optimize the parameters of the drilling tool itself. The cutting tool used in the milling process affects performance, and the research seeks to determine the effect of tool geometry, length, and stiffness of the tool. Receptance Coupling Substructure Analysis (RCSA) is a technique applied to predict the dynamic response of a milling tool and its holder when subjected to cutting forces and spindle vibrations. Along with choosing the tool selection, when the cutting operation happens, the cutting force and speed affect the stability of the tool. This previous research and calculations have been utilized to create milling stability models. Due to the

uncertainty of cutting forces, the stability models use a Monte Carlo simulation to account for the uncertainty of the milling process. This research is focused on a milling stability model on an aluminum workpiece. The simulated model created includes 10,000 simulated data iterations with varying axial depth of the tool and rotation speed. Each simulation has four parameters connected to the stability graph. The beta matrix is the angle of the tool on the workpiece surface (deg). The Kolmogorov-Smirnov (KS) matrix is the force model coefficient K_s (N/mm2). The (KTF) matrix is force stiffness k (N/rad). The CFT matrix is the connection damping c (N-s/rad). The goal of previous stability mapping was to identify the combinations of parameters such as spindle speed, feed rate, and depth of axial cut that result in the stable operation of a machine; whereas, for this project stability lobes will be used to better visualize the stability boundary line and to analyze the two stability testing methods based on point selections using a machine learning (ML) model.

Goals

The graphed simulated stability lobe diagrams may be partitioned using real-world tests also known as ground truths in this study to determine which iterations are stable and which are not compared to the ground truths point (x, y) coordinate placement on the diagram. The tool rotations and axial depth mapped in the stability lobe diagram are visualized to show stable combinations. This research aims to enhance the analysis process to select a more accurate, cost-efficient test for stability and reduce the number of tests necessary to find the optimal stability line and stopping criteria for testing. Using previous literary works on identifying the stable and unstable boundary line in the milling process, this research will take the point stability identification testing

a step further using ML to compare the current capabilities of testing sequentially versus combinations of points all at once. In addition to optimizing the testing point selection process, the ML SHAP model will be provided points and two testing methods to identify the accuracy of these tests and point selections. Then, the model will be provided with the costs of material, time, and monetary expenses to confirm if the two tests have respective advantages and to what extent. The model will be given 24 ground truth points and provide the percentage eliminated from the 10,000 simulated data iterations based on its limited real-world testing inputs to determine which of the two testing methods is more efficient with the performance of elimination and the most cost-effective regarding the amount materials used in the milling process, expenses of materials used, and time.

Data Gaps

The dataset in use has some notable gaps. Labeling gaps are the main concern as we only have 24 labeled real-world tests. The gap is that the true boundary between stable and unstable is unknown. The information gleaned from between certain points means a matter of stability as this boundary line is only approximately known and not strictly identified. This project aims to better improve the clarity between the labeled test points, their stability, and the 10,000 iterations by comparing the two testing methods to determine the more effective option.

This is in addition to research focusing on optimizing the partitioning process for stability mapping by strategically selecting test points and reducing the number of experimental tests required. These techniques aim to efficiently explore the parameter space and identify critical test point selections to optimize the output for stable milling conditions.

Chapter 2

Literature Review

Previous Research

Researchers have investigated the effects of tool geometry, length, material, and stiffness on milling performance and stability. Research has explored optimal tool designs to minimize vibrations and improve material removal rates (MRR), finding optimal tooling length and stiffness parameters. Other research has focused on developing accurate models to predict cutting forces during milling operations. These models consider factors such as tool geometry, material properties, cutting parameters, and machine dynamics to estimate the forces acting on the tool. Researchers have developed analytical and numerical models to predict milling stability and identify conditions that lead to chatter [1]. These models often consider factors like spindle speed, axial depth of cut, tool geometry, cutting parameters, and machine dynamics to determine stable cutting conditions [2]. Monte Carlo simulation techniques have been used to account for uncertainties in the milling process, such as variations in material properties, tool wear, and cutting conditions [3]. These simulations help to assess the robustness of stability predictions and optimize milling parameters under uncertain conditions. The RCSA method, introduced by Schmitz et al., has been widely studied for predicting tool-tip receptance and coupling tool-holder dynamics with machine tool structures [4]. This approach allows for more accurate stability predictions by considering the dynamic interaction between the tool, holder, and machine. Many research studies have conducted experimental tests to validate stability models and simulation results. These experiments

involve measuring cutting forces, tool vibrations, surface roughness, and other parameters to assess the stability of the milling process under different conditions [5].

Chapter 3

Materials and Methods

Data Collection

Stability Limit Matrix

The data used in this research is created by a milling stability model. The stability model uses a Monte Carlo simulation to account for the uncertainty of the milling process. The ground truths are 24 real-world tests done by Schmitz with nearly identical parameters to the simulations [4].

Fig. 1 found in the appendix displays simplified 10 out of 10,000 simulated data iterations produced by the simulation represented as blue lines along with the labeled 1 through 24 ground truths displayed as red x's and green circles depending on the point's specified stability. The green circles are stable points within the stability map. Meanwhile, the red x's signify unstable points being affected by chatter. Please note that the plotted lines of the stability limit matrices within this report do continue before the 6600 spindle speed and after the 10,600 spindle speed; however, for this report, the continuations past these x-axis ranges are not plotted to emphasize the limited range this project takes into consideration.

Fig. 2 in the appendix displays the 10,000 sample data iterations produced by simulations on the Stability Lobe Diagram. Fig. 3 in the appendix displays the Stability Table dataset and Fig. 4 in the appendix labels the ground truths and their stability.

Stability Map

For each unstable point, it is certain that everything above that point is also unstable; whereas, there is not much to glean for certain about the points below as they

could be either stable or unstable. For each stable point, it is certain that everything under that point is also stable; whereas, there is not much known for certain about the points above as they could either continue being stable or become unstable. Since the true stability boundary is unknown, the 24 ground truths are used to test which of the 10,000 lines are to be considered stable or unstable at the point's specific axial depth and rpm. Fig. 5 in the appendix labels each row as either true denoting stable or false denoting unstable within the specific RPM ranges at axial depths from 1 mm to 4 mm. Fig. 6 in the appendix displays the count of rows where true means rows are at or above the point and false means rows are below the point per RPM and axial depth ranges along with their respective percentages of unstable rows. The model iterates over two different methodologies of the order involved with selecting point(s) that maximize the elimination of unstable rows and optimize the performance of point testing. This testing can be done using two different methods: Sequencing and Combination.

Sequencing

Sequencing involves selecting one point at a time from the 24 ground truths that have the best performance value based on the percentage of the 10,000 rows that are eliminated due to the point being unstable. Once the first best point has been determined it is set or locked in as the first testing point. From there, all the corresponding rows from the 10,000 that were deemed unstable and eliminated from the first best point are then removed from the data to avoid row overlap in the next best point selection. Overlap is when a row that one point eliminates is also to be eliminated by another point(s). To avoid this, each unstable point has a listed set of all rows that are at or above the specified point since it is known that these will also be in the unstable range. By using union sets

and intersections, it is possible to compare each point to determine and eliminate the overlapping rows. For the next best point selection, the dataset is then updated with the new performance values based on the remaining percentage of the 10,000 rows that are to be eliminated. This process continues until the stopping criteria is reached which is either when there are no more points to select as the next best point due to no more rows remaining to be eliminated or there is little to no increase in the total row elimination performance value. The stopping criteria can be determined by whichever comes first as the first route means the testing process cannot be continued due to a lack of remaining unstable rows while the latter involves the testing process not being enhanced enough to continue with tests after a certain point due to no value added.

Combination

Combination testing involves selecting multiple points at a time from the 24 ground truths. This process begins by finding all possible combinations of 2 points (24C2), 3 points (24C3), ..., and 6 points (24C6) without repetition. For instance, there are 276 possible combinations for selecting 24C2 to 134,596 possible combinations for selecting 24C6. Overlap between rows is also prevalent in this method, so union combinations are also taken into account to avoid any overlapped rows between the point combination results. After this, the produced combinations are sorted to reveal the best point combinations based on the performance of unstable row elimination from the 10,000 simulations. This process can be continued until the stopping criteria are reached which is either when there are no more points to select as no more of the ground truths remain to be selected after 24C24 or there is little to no increase in the total row elimination performance value as the combinations of points increase. The stopping

criteria can be determined by whichever comes first as the first route means the testing process cannot be continued due to a lack of remaining unique points to select while the latter involves the testing process not being enhanced enough to continue with tests after a certain point due to no value added.

Parameters

- Beta matrix is the angle of the tool on the workpiece surface (deg).
- KS matrix is the force model coefficient K_s (N/mm2).
- KTF matrix is force stiffness k (N/rad).
- CFT matrix is the connection damping c (N-s/rad).
- RPM is the rotation speed of the tool in revolutions per minute.
- Axial depth is the tool deepness into the workpiece in mm.

Equations

Equation (1)

Equation (1) is used to determine the percent of performance as defined in Eq. 1. The symbol n indicates the number of unstable rows eliminated by a specific point or combination of points, N is the 10,000 simulations, and P represents the performance of unstable row eliminations as a percentage.

$$P = \frac{n}{N} \times 100 \quad (1)$$

Equation (2)

Equation (2) is used to determine the number of combinations between the total number of items in a set, n, and the number of unique arrangements, r, as shown in Eq. 2, which C stands for combinations.

$$ {}_nC_r = \frac{n!}{r! \times (n-r)!} \quad (2) $$

Equation (3)

Equation (3) is a union of two sets listing all elements from both sets defined in Eq. 3. The symbol A represents a ground truth point being compared to B a different ground truth point.

$$ |A \cup B| = |A| + |B| - |A \cap B| \quad (3) $$

Equation (4)

Equation (4) is an intersection of two sets listing only elements contained in both sets defined in Eq. 4. The symbol A represents a ground truth point being compared to B a different ground truth point.

$$ |A \cap B| = |A| + |B| - |A \cup B| \quad (3) $$

Equation (5)

Equation (5) is used to determine the material removal rate MRR defined in Eq. 5. The symbol D indicates the depth of cut, W is the width of cut, and F represents the feed rate.

$$ MRR = \frac{D \times W \times F}{1000} \quad (5) $$

Data Analysis Techniques

By leveraging ML models, research can be enhanced in the analysis of the partitioning process, identification of unstable rows from stability tests, and reduction of the number of tests required to characterize stability accurately. Additionally, these models can provide insights into the underlying relationships between input parameters and stability outcomes, contributing to a deeper understanding of the milling process.

Ensemble methods like Random Forests (RF) can be utilized to improve the accuracy of decision tree-based approaches. The model is trained on simulated axial depths, ground truth RPM values, and stability. SHapley Additive exPlanations known as SHAP can then be used to analyze the data output and explain connections between input parameters. SHAP values also take into account the impact on the parameters' contributions to the output and rank the measurements of each featured value from high to low.

Chapter 4

Results and Discussion

After the simulated test data is collected through sequencing and combination methods, it is used within SHAP to provide more insight into the two testing methods through performance and row elimination counts. The models' point rankings are tabled for their performance which is optimized to show the best testing point selections based on percent eliminated and a cost analysis. The two methods yielded identical point selection and performance results. One thing to note is that the combination testing method used less computational time for testing smaller numbers of points; however, the sequencing method used less computational time for testing larger numbers of points.

Data Results

The computational time of selecting points and accurately listing the performance of each selected point is compared to judge the effectiveness of the two testing methods.

1st Best Point Sequence Output

Fig. 7 in the appendix displays each point's list of unstable row sets. There is a total of 9 points with sets of unstable rows. Please note that although some points may be considered unstable, they may not have any values in their row sets due to none of the 10,000 iterations being at or above the point. As for the stable points, they are not considered since the objective is to eliminate all unstable row sets using the least amount of point selection tests. Fig. 8 in the appendix lists the first best sequence of points based on their performance of unstable row eliminations. The sequencing method for selecting the first best point produced the result of point 16 as it has the highest performance rating.

2nd Best Point Sequence Output

Fig. 9 in the appendix displays each point's updated list of unstable row sets after using union sets to remove unstable row overlap from point 16. The number of points with unstable rows has decreased to only 3 sets. Fig. 10 in the appendix lists the second-next-best sequence of points based on their performance of unstable row eliminations. The sequencing method for selecting the second next-best point produced the result of point 6 as it has the highest performance rating after updating the dataset to remove rows that overlap with the first-best point of 16.

3rd Best Point Sequence Output

Fig. 11 in the appendix displays each point's updated list of unstable row sets after using union sets to remove unstable row overlap from point 6. The number of points with unstable rows has decreased to only 3 sets. Fig. 12 in the appendix lists the third-next-best sequence of points based on their performance of unstable row eliminations. The sequencing method for selecting the third next-best point produced the result of point 23 as it has the highest performance rating after updating the dataset to remove rows that overlap with the second-best point of 6.

4th Best Point Sequence Output

Fig. 13 in the appendix displays each point's updated list of unstable row sets after using union sets to remove unstable row overlap from point 23. The number of points with unstable rows has now decreased to 0 sets. Fig. 14 in the appendix lists the output of the fourth-next-best sequence of points based on their performance of unstable row eliminations. The sequencing method for selecting the fourth next-best point produced the result of all points having a performance rating of 0% after updating the

dataset to remove rows that overlap with the third-best point of 23. The lack of unstable point row sets remaining means that the stopping criteria have been met for this sequence. Fig. 15 in the appendix displays this method's sequencing output of best point selections.

24C1 Output

Fig. 16 in the appendix displays the 24 C 1 combinations of the 24 different possible combinations without repetition. Each point's performance is denoted by its elimination of unstable rows from the 10,000 iterations at or above the point. As for the stable points, they are not considered since the objective is to eliminate all unstable row sets using the least amount of point selection tests. The combination method for selecting the top one point produced the result of point 16 as it has the highest performance rating.

24C2 Output

Fig. 17 in the appendix displays the 24 C 2 combinations of the 276 different possible combinations without repetition. Each combination of 2 points has an updated list of performances based on the removal of the overlap from the 2 points' combinations by using intersections and unions of the unstable rows from the 2 points' sets. The combination method for selecting the two best points produced the result of points 6 and 16 as this combination has the highest performance rating after updating the dataset to ensure that rows that overlap between each combination of points were only counted toward one of the points and not both.

24C3 Output

Fig. 18 in the appendix displays the 24 C 3 combinations of the 2,024 different possible combinations without repetition. Each combination of 3 points has an updated

list of performances based on the removal of the overlap from the 3 points' combinations by using intersections and unions of the unstable rows from the 3 points' sets. The combination method for selecting the three best points produced the result of points 6, 16, and 23 as this combination has the highest performance rating after updating the dataset to ensure that rows that overlap between each combination of points were only counted toward one of the points and not all three.

24C4 Output

Fig. 19 in the appendix displays the 24 C 4 combinations of the 10,626 different possible combinations without repetition. Each combination of 4 points has an updated list of performances based on the removal of the overlap from the 4 points' combinations by using intersections and unions of the unstable rows from the 4 points' sets. The combination method for selecting the four best points produced the result of points 2, 6, 16, and 23. Though this is claimed to be the combination with the highest performance rating after updating the dataset to ensure that rows that overlap between each combination of points were only counted toward one of the points and not all four, it is imperative to check the performance column and note that the values are equal. The lack of changes to the first performance percentage means that the stopping criteria have been met for this combination as there are no longer any points that add value to the testing. To further emphasize this, Fig. 20 in the appendix displays the 24 C 5 combinations of the 42,504 different possible combinations without repetition and Fig. 21 in the appendix displays the 24 C 6 combinations of the 134,596 different possible combinations without repetition. Both of these combinations further prove that the performance no longer

changes with more combinations of points selected. The performance levels out of 53.7% beginning at 24 C 3 being the least amount of point selections required for testing.

Analysis of Results

The results show that both testing methods produce viable and identical results of point selections. Both methods of testing showed identical point selection results backed by their performance of eliminating unstable rows; however, there are good and bad qualities of both testing methods. The sequencing testing method appears the most effective when wanting a larger sequence of best testing points as it takes much less computational time due to not having to do all the different combinations the other method requires. The combination testing method appears the most effective when using a lower value of the combination's point group values due to a more rapid computational time and it requires less input from the operator as required by the sequencing method where the dataset had to be updated after each point selection. Combination testing to determine the best selection of testing points can be used to select any grouping of points and produce performance results without having to go one by one as with sequencing. However, with combinations, I found myself having to run it one extra time to confirm if the stopping criteria were met or not as opposed to sequencing which provides the remaining performance percentages from each point beneath the latest point’s selection.

The selection order of tests matters since the objective is to use the least amount of points for testing. We can use both testing methods to identify the best order of selected test points that eliminates the highest amount of rows from the 10,000 data iterations varies based on the testing method, but it does vary based on the testing method. The combination testing order is produced all at once for testing the point(s), so

as long as each selected point is tested, the order should not matter. However, for sequencing, the testing order must be done sequentially since we test one at a time. Both testing methods showed that when using the output best test point(s) selections, the partitioning process is significantly more efficient than randomly testing points.

When estimating the best stopping criterion, predictions are not being enhanced enough to warrant continuing with tests after a certain point as the tests are providing nearly no value added, and the effort to run the model outweighs the added value. The stopping criterion can vary based on the circumstances of the testing methods; however, it can be noted that after 2 point selection tests, there was a performance of 53.68%, and after 3 tests the performance only increased by 0.02% based on only 2 unstable rows being eliminated with the selection of this third best point, and after the 4th test there was no change in performance for either testing method. The model's performance did not significantly increase after adding more tests after this point.

Both testing methods agree that when the effort to run the model outweighs the added value the stopping criteria have been met. This means the percentage improvement no longer outweighs the expenses of time, materials used, and money it takes to run the experiment. Both testing methods have the same output performance accuracy, the same materials used from MRR, expenses of materials used. Fig. 22 in the appendix displays the MRR and cost of testing for each point which further proves that both testing methods cost the same and use the same amount of material from the example workpiece of a 6061-T6 aluminum block when there are 4 teeth and the feed per tooth is 0.1 mm/tooth. The only difference between the sequencing and combination methods is the cost of time and ease of testing multiple points at once.

1st Best Point Sequence Output

The sequencing method for selecting the first best point produced the result of point 16 as it has the highest performance rating of 47.23%.

2nd Best Point Sequence Output

The sequencing method for selecting the second next-best point produced the result of point 6 as it has the highest performance rating of 6.45%.

3rd Best Point Sequence Output

The sequencing method for selecting the third next-best point produced the result of point 23 as it has the highest performance rating of 0.02%.

24C1 Output

The combination method for selecting the top one points produced the result of point 16 as it has the highest performance rating of 47.23%.

24C2 Output

The combination method for selecting the two best points produced the result of points 6 and 16 as it has the highest performance rating of 53.68%.

24C3 Output

The combination method for selecting the three best points produced the result of points 6, 16, and 23 as it has the highest performance rating of 53.70%.

SHAP Output

SHAP produced Fig. 23 found in the appendix displaying the correlation between the RPM range, axial depths, and stability from each point. The featured values are the RPM ranges denoted by X and the axial depths denoted by Y. Each row iteration is shown as a dot beside each RPM range all with varied colors based on the featured value

scale. The greater the feature value, the higher it is on the featured value color scale denoted by a red hue; whereas, the lower the feature value, the lower it is denoted by a blue hue. Any feature value between the two ranges is denoted by the purple shade between the two red and blue colors of the feature value scales. The SHAP values show that anything on the left of the graph has a negative correlation, while anything on the right has a positive correlation. Stable feature values are on the left side while unstable ones are on the right. The greater the feature value of Y, there tends to be a positive effect on the output of stability being unstable. The lower the feature value of Y, there tends to be a negative effect on the output of stability being stable. This means that with higher axial depths, there tends to be more instability. The greater the feature value of X, there tends to be a negative effect on the output of stability being stable. The lower the feature value of X, there tends to be a positive effect on the output of stability being unstable. This means that with higher RPM ranges, there tends to be more stability. Since the Y feature value is plotted on the top of the summary output, that means that axial depth has the most impact on the model's output of stability. This plot helps with visualizing how each iteration tends to be either stable or unstable and how axial depths and RPM ranges play a key role in the correlation as well.

Chapter 5

Conclusions and Recommendations

Different iterations could be simulated to further determine the most optimal method of testing. Since the methodology was only tested with one dataset, the results could differ with a larger dataset since the sequencing method could produce distinct results as it tests a different route than the combination method does. Expanding on the criterion for test points such as material removal and cost per test could be explored. Further research could be done by taking these testing points and exploring ML predicting the MRR and cost per test at randomized points to see if the predictions align and if the MRR and expenses further impact the best testing points on a larger scale. The ML route to predict stability without ground truths is another expansion of this project that could be further explored. SHAP can help with this further expansion by reading in all points instead of just the known unstable ones. With the future expansion of the project using SHAP, more features aside from axial depths and RPMs can still be added to explore should they become more apparent with a different, larger dataset. The ML SHAP tool has promising results in its ability to analyze the sequencing and combination testing methods and produce viable insight into the dataset.

References

[1] Turner, D. S. (2011). Process Damping Parameters. IOP Conference Series. Materials Science and Engineering, 26(1), 12008–12018. https://doi.org/10.1088/1757-899X/26/1/012008.

[2] Shaik, J. H., Mutra, R. R., Galal, A. M., & Tanneeru, S. R. (2022). Investigation of chatter prediction in end milling using morphological studies on aluminum alloy (Al6061). Noise & Vibration Worldwide, 53(4–5), 233–243. https://doi.org/10.1177/09574565221093232.

[3] Dou, J., Dong, H., Zhang, J., Meng, J., Tian, Y., Pang, M., Luo, W., & Xu, C. (2023). An adaptive method of measuring the rake face wear of end mills based on Image Feature Point set registration. Journal of Manufacturing Processes, 98, 149–158. https://doi.org/10.1016/j.jmapro.2023.05.027.

[4] Karandikar, J., & Schmitz, T. (2024). (rep.). Uncertainty reduction in milling stability modeling by sample partitioning and Bayesian inference. Knoxville, Tennessee. Article in press.

[5] Shi, M., Qin, X., Li, H., Shang, S., Jin, Y., & Huang, T. (2020). Cutting force and chatter stability analysis for PKM-based helical milling operation. International Journal of Advanced Manufacturing Technology, 111(11–12), 3207–3224. https://doi.org/10.1007/s00170-020-06252-3.

[6] Titu, N. A., Baucum, M., No, T., Trotsky, M., Karandikar, J., Schmitz, T. L., & Khojandi, A. (2021). Estimating Johnson-cook material parameters using neural networks. Procedia Manufacturing, 53, 680–689. https://doi.org/10.1016/j.promfg.2021.06.082.

[7] Cherukuri, H., Perez-Bernabeu, E., Selles, M., & Schmitz, T. (2019). Machining chatter prediction using a data learning model. Journal of Manufacturing and Materials Processing, 3(2), 45. https://doi.org/10.3390/jmmp3020045.

[8] Karandikar, J., Honeycutt, A., Schmitz, T., & Smith, S. (2020). Stability boundary and optimal operating parameter identification in milling using Bayesian learning. Journal of Manufacturing Processes, 56, 1252–1262. https://doi.org/10.1016/j.jmapro.2020.04.019.

Appendix

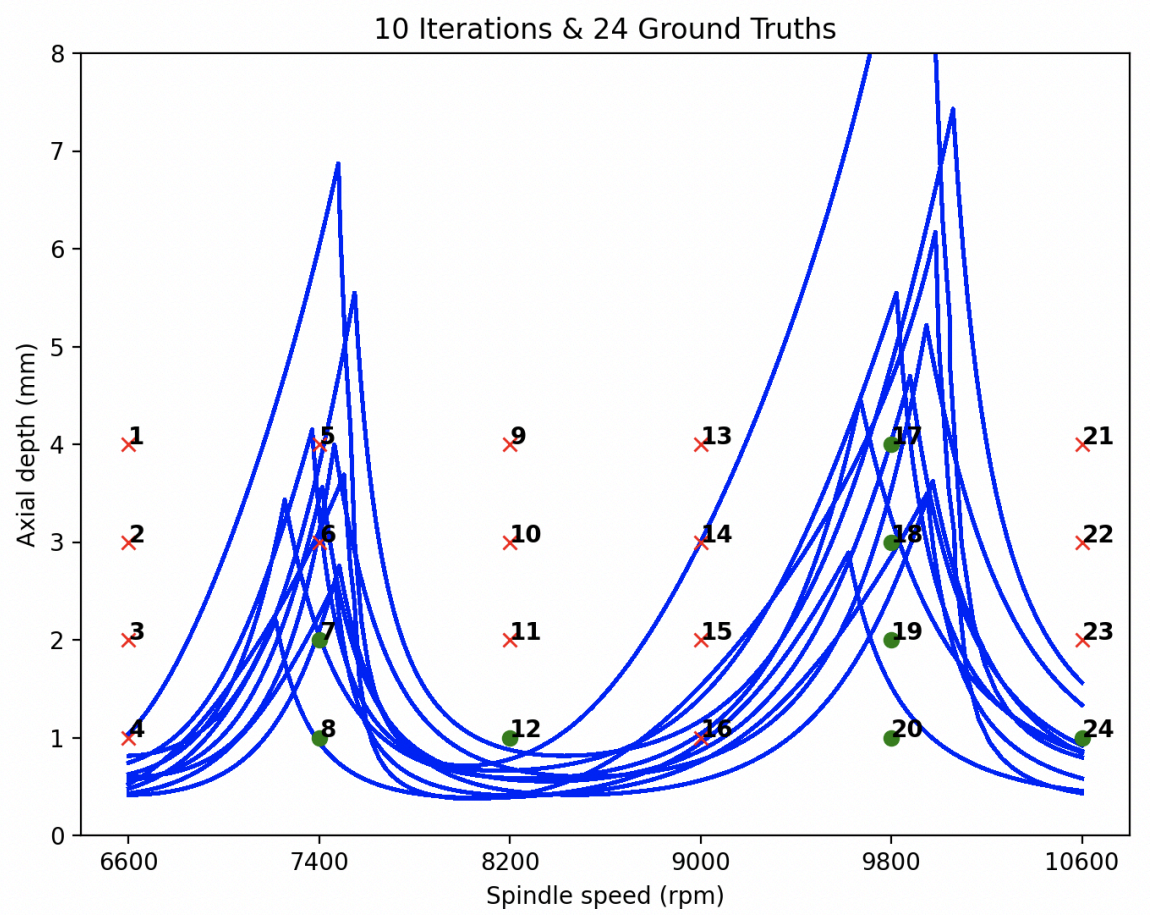


Figure 1. Simplified Stability Limit Matrix showing 10 lines out of the 10,000.

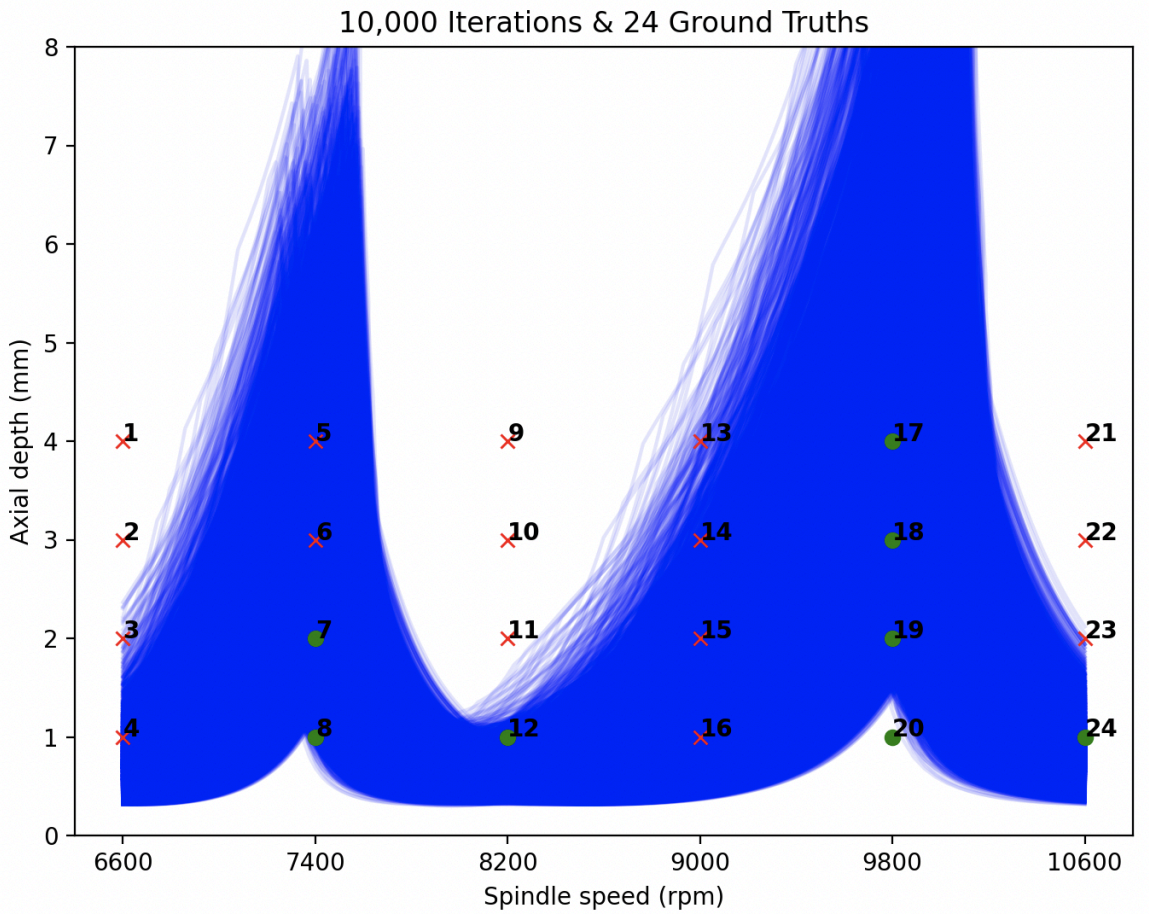


Figure 2. Stability Limit Matrix of Entire 10,000 Lines.

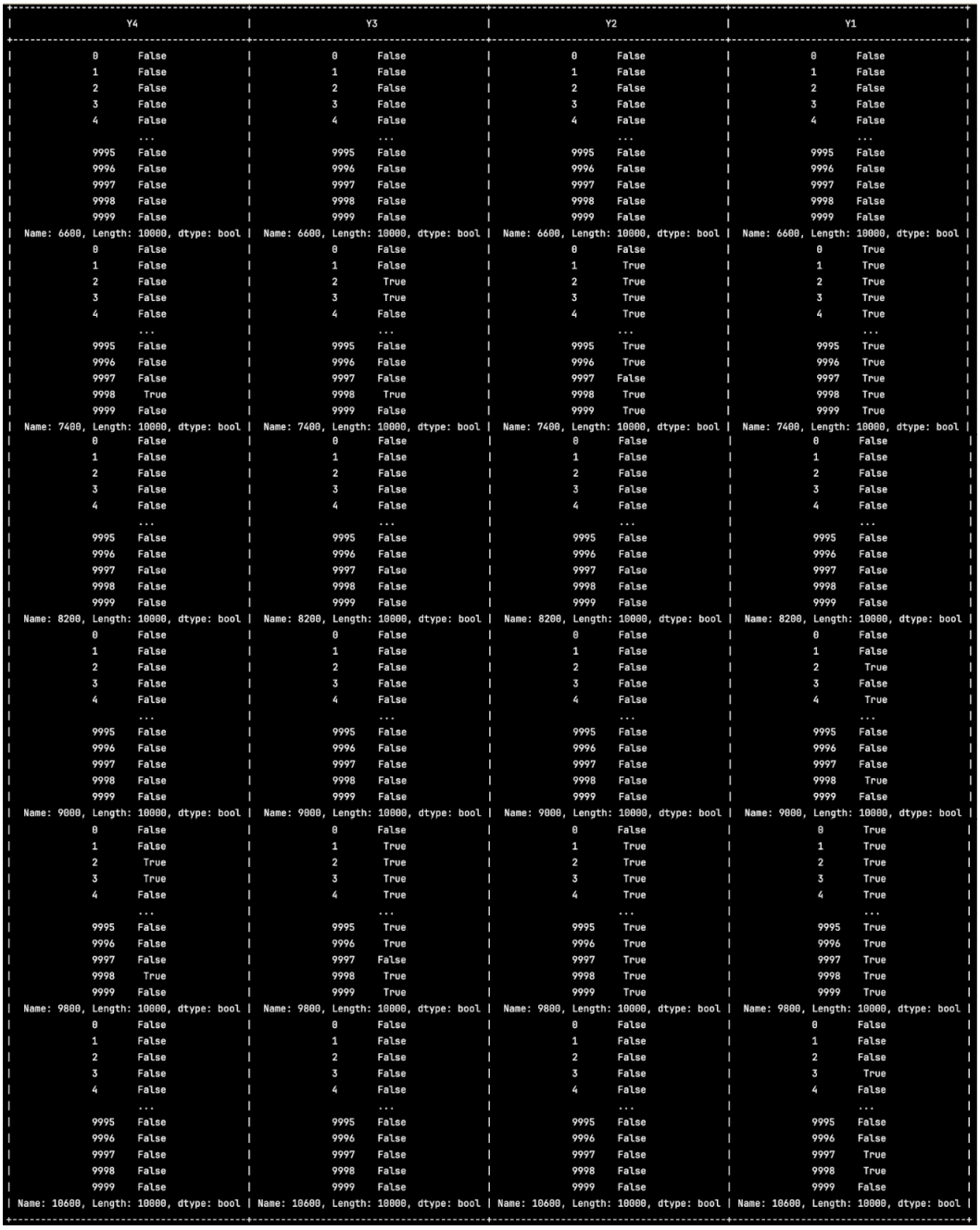
	6600	6601	6602	6603	...	10598	10599	10600	Row Label
0	0.34232	0.34220	0.34208	0.34196	...	0.83717	0.83587	0.83457	1
1	0.47397	0.47422	0.47447	0.47474	...	0.71791	0.71695	0.71600	2
2	0.49917	0.50026	0.50135	0.50246	...	0.45806	0.45757	0.45707	3
3	0.64437	0.64459	0.64485	0.64510	...	1.13240	1.13100	1.12960	4
4	0.42721	0.42813	0.42904	0.42996	...	0.40219	0.40178	0.40137	5
...	...	...	...	...	...	...	...	...	...
9995	0.49499	0.49550	0.49602	0.49653	...	0.58856	0.58806	0.58756	9996
9996	0.51593	0.51643	0.51694	0.51746	...	0.63739	0.63670	0.63601	9997
9997	0.42811	0.42793	0.42774	0.42756	...	1.01750	1.01580	1.01410	9998
9998	0.72479	0.72524	0.72570	0.72616	...	1.07100	1.06980	1.06860	9999
9999	0.51254	0.51263	0.51273	0.51282	...	0.94473	0.94341	0.94209	10000

[10000 rows x 4002 columns]

Figure 3. Stability Table with Labeled Rows.

	Point	X	Y	Stability
0	P1	6600	4	Unstable
1	P2	6600	3	Unstable
2	P3	6600	2	Unstable
3	P4	6600	1	Unstable
4	P5	7400	4	Unstable
5	P6	7400	3	Unstable
6	P7	7400	2	Stable
7	P8	7400	1	Stable
8	P9	8200	4	Unstable
9	P10	8200	3	Unstable
10	P11	8200	2	Unstable
11	P12	8200	1	Stable
12	P13	9000	4	Unstable
13	P14	9000	3	Unstable
14	P15	9000	2	Unstable
15	P16	9000	1	Unstable
16	P17	9800	4	Stable
17	P18	9800	3	Stable
18	P19	9800	2	Stable
19	P20	9800	1	Stable
20	P21	10600	4	Unstable
21	P22	10600	3	Unstable
22	P23	10600	2	Unstable
23	P24	10600	1	Stable

Figure 4. Ground Truths with Stability Labeled.



Y4		Y3		Y2		Y1	
0	False	0	False	0	False	0	False
1	False	1	False	1	False	1	False
2	False	2	False	2	False	2	False
3	False	3	False	3	False	3	False
4	False	4	False	4	False	4	False
	...		...		...		...
9995	False	9995	False	9995	False	9995	False
9996	False	9996	False	9996	False	9996	False
9997	False	9997	False	9997	False	9997	False
9998	False	9998	False	9998	False	9998	False
9999	False	9999	False	9999	False	9999	False
Name: 6600, Length: 10000, dtype: bool		Name: 6600, Length: 10000, dtype: bool		Name: 6600, Length: 10000, dtype: bool		Name: 6600, Length: 10000, dtype: bool	
0	False	0	False	0	False	0	True
1	False	1	False	1	True	1	True
2	False	2	True	2	True	2	True
3	False	3	True	3	True	3	True
4	False	4	False	4	True	4	True
	...		...		...		...
9995	False	9995	False	9995	True	9995	True
9996	False	9996	False	9996	True	9996	True
9997	False	9997	False	9997	False	9997	True
9998	True	9998	True	9998	True	9998	True
9999	False	9999	False	9999	True	9999	True
Name: 7400, Length: 10000, dtype: bool		Name: 7400, Length: 10000, dtype: bool		Name: 7400, Length: 10000, dtype: bool		Name: 7400, Length: 10000, dtype: bool	
0	False	0	False	0	False	0	False
1	False	1	False	1	False	1	False
2	False	2	False	2	False	2	False
3	False	3	False	3	False	3	False
4	False	4	False	4	False	4	False
	...		...		...		...
9995	False	9995	False	9995	False	9995	False
9996	False	9996	False	9996	False	9996	False
9997	False	9997	False	9997	False	9997	False
9998	False	9998	False	9998	False	9998	False
9999	False	9999	False	9999	False	9999	False
Name: 8200, Length: 10000, dtype: bool		Name: 8200, Length: 10000, dtype: bool		Name: 8200, Length: 10000, dtype: bool		Name: 8200, Length: 10000, dtype: bool	
0	False	0	False	0	False	0	False
1	False	1	False	1	False	1	False
2	False	2	False	2	False	2	True
3	False	3	False	3	False	3	False
4	False	4	False	4	False	4	True
	...		...		...		...
9995	False	9995	False	9995	False	9995	False
9996	False	9996	False	9996	False	9996	False
9997	False	9997	False	9997	False	9997	False
9998	False	9998	False	9998	False	9998	True
9999	False	9999	False	9999	False	9999	False
Name: 9000, Length: 10000, dtype: bool		Name: 9000, Length: 10000, dtype: bool		Name: 9000, Length: 10000, dtype: bool		Name: 9000, Length: 10000, dtype: bool	
0	False	0	False	0	False	0	True
1	False	1	True	1	True	1	True
2	True	2	True	2	True	2	True
3	True	3	True	3	True	3	True
4	False	4	True	4	True	4	True
	...		...		...		...
9995	False	9995	True	9995	True	9995	True
9996	False	9996	True	9996	True	9996	True
9997	False	9997	False	9997	True	9997	True
9998	True	9998	True	9998	True	9998	True
9999	False	9999	True	9999	True	9999	True
Name: 9800, Length: 10000, dtype: bool		Name: 9800, Length: 10000, dtype: bool		Name: 9800, Length: 10000, dtype: bool		Name: 9800, Length: 10000, dtype: bool	
0	False	0	False	0	False	0	False
1	False	1	False	1	False	1	False
2	False	2	False	2	False	2	False
3	False	3	False	3	False	3	True
4	False	4	False	4	False	4	False
	...		...		...		...
9995	False	9995	False	9995	False	9995	False
9996	False	9996	False	9996	False	9996	False
9997	False	9997	False	9997	False	9997	True
9998	False	9998	False	9998	False	9998	True
9999	False	9999	False	9999	False	9999	False
Name: 10600, Length: 10000, dtype: bool		Name: 10600, Length: 10000, dtype: bool		Name: 10600, Length: 10000, dtype: bool		Name: 10600, Length: 10000, dtype: bool	

Figure 5. RPM Ranges Labeled True (Stable) & False (Unstable) at Specific Axial Depths.

```
Results for 6600:
Y4: True=0, False=10000, Percentage=0.00
Y3: True=0, False=10000, Percentage=0.00
Y2: True=13, False=9987, Percentage=0.13
Y1: True=869, False=9131, Percentage=8.69

Results for 7400:
Y4: True=1376, False=8624, Percentage=13.76
Y3: True=3626, False=6374, Percentage=36.26
Y2: True=7429, False=2571, Percentage=0.00
Y1: True=9933, False=67, Percentage=0.00

Results for 8200:
Y4: True=0, False=10000, Percentage=0.00
Y3: True=0, False=10000, Percentage=0.00
Y2: True=0, False=10000, Percentage=0.00
Y1: True=227, False=9773, Percentage=0.00

Results for 9000:
Y4: True=35, False=9965, Percentage=0.35
Y3: True=277, False=9723, Percentage=2.77
Y2: True=1382, False=8618, Percentage=13.82
Y1: True=4723, False=5277, Percentage=47.23

Results for 9800:
Y4: True=3772, False=6228, Percentage=0.00
Y3: True=6483, False=3517, Percentage=0.00
Y2: True=9312, False=688, Percentage=0.00
Y1: True=10000, False=0, Percentage=0.00

Results for 10600:
Y4: True=0, False=10000, Percentage=0.00
Y3: True=0, False=10000, Percentage=0.00
Y2: True=2, False=9998, Percentage=0.02
Y1: True=2468, False=7532, Percentage=0.00
```

Figure 6. Count of RPM Ranges Labeled True (Rows At or Above Count) & False (Rows Below Count) at Specific Axial Depths With Percentage of Unstable Rows.

List Unstable Row Sets

	Point	Rows	Stability
0	P1	[]	Unstable
1	P2	[]	Unstable
2	P3	[338, 1614, 2184, 2194, 2264, 3124, 3661, 4139...	Unstable
3	P4	[17, 19, 28, 31, 38, 50, 70, 74, 78, 88, 94, 1...	Unstable
4	P5	[17, 19, 22, 24, 26, 31, 34, 38, 47, 50, 51, 5...	Unstable
5	P6	[2, 3, 8, 9, 11, 17, 18, 19, 22, 23, 24, 26, 2...	Unstable
6	P7	[]	Stable
7	P8	[]	Stable
8	P9	[]	Unstable
9	P10	[]	Unstable
10	P11	[]	Unstable
11	P12	[]	Stable
12	P13	[70, 78, 338, 714, 2059, 2171, 2184, 2264, 228...	Unstable
13	P14	[17, 28, 31, 34, 53, 70, 74, 78, 116, 124, 144...	Unstable
14	P15	[17, 22, 28, 31, 32, 34, 38, 50, 51, 53, 70, 7...	Unstable
15	P16	[2, 4, 8, 9, 11, 12, 17, 18, 19, 20, 21, 22, 2...	Unstable
16	P17	[]	Stable
17	P18	[]	Stable
18	P19	[]	Stable
19	P20	[]	Stable
20	P21	[]	Unstable
21	P22	[]	Unstable
22	P23	[3797, 5410]	Unstable
23	P24	[]	Stable

Figure 7. List of Unstable Row Sets Used for Determining Sequencing's First Best Point.

1st Best Sequence		
	Point	Performance
15	P16	47.23
5	P6	36.26
14	P15	13.82
4	P5	13.76
3	P4	8.69
13	P14	2.77
12	P13	0.35
2	P3	0.13
22	P23	0.02
21	P22	0.00
20	P21	0.00
19	P20	0.00
18	P19	0.00
17	P18	0.00
16	P17	0.00
0	P1	0.00
1	P2	0.00
11	P12	0.00
10	P11	0.00
9	P10	0.00
8	P9	0.00
7	P8	0.00
6	P7	0.00
23	P24	0.00

Figure 8. Sequencing's First Best Point Selection With Performance Percentages.

List Unstable Row Sets ----------

	Point	Rows	Stability
0	P1	[]	Unstable
1	P2	[]	Unstable
2	P3	[]	Unstable
3	P4	[]	Unstable
4	P5	[8832, 1145, 7690, 2321, 5522, 3219, 1912, 667...	Unstable
5	P6	[8192, 3, 6151, 4105, 2066, 6164, 23, 2071, 61...	Unstable
6	P7	[]	Stable
7	P8	[]	Stable
8	P9	[]	Unstable
9	P10	[]	Unstable
10	P11	[]	Unstable
11	P12	[]	Stable
12	P13	[]	Unstable
13	P14	[]	Unstable
14	P15	[]	Unstable
16	P17	[]	Stable
17	P18	[]	Stable
18	P19	[]	Stable
19	P20	[]	Stable
20	P21	[]	Unstable
21	P22	[]	Unstable
22	P23	[5410, 3797]	Unstable
23	P24	[]	Stable

Figure 9. List of Unstable Row Sets Remaining Used for Determining Sequencing's Second Next Best Point.

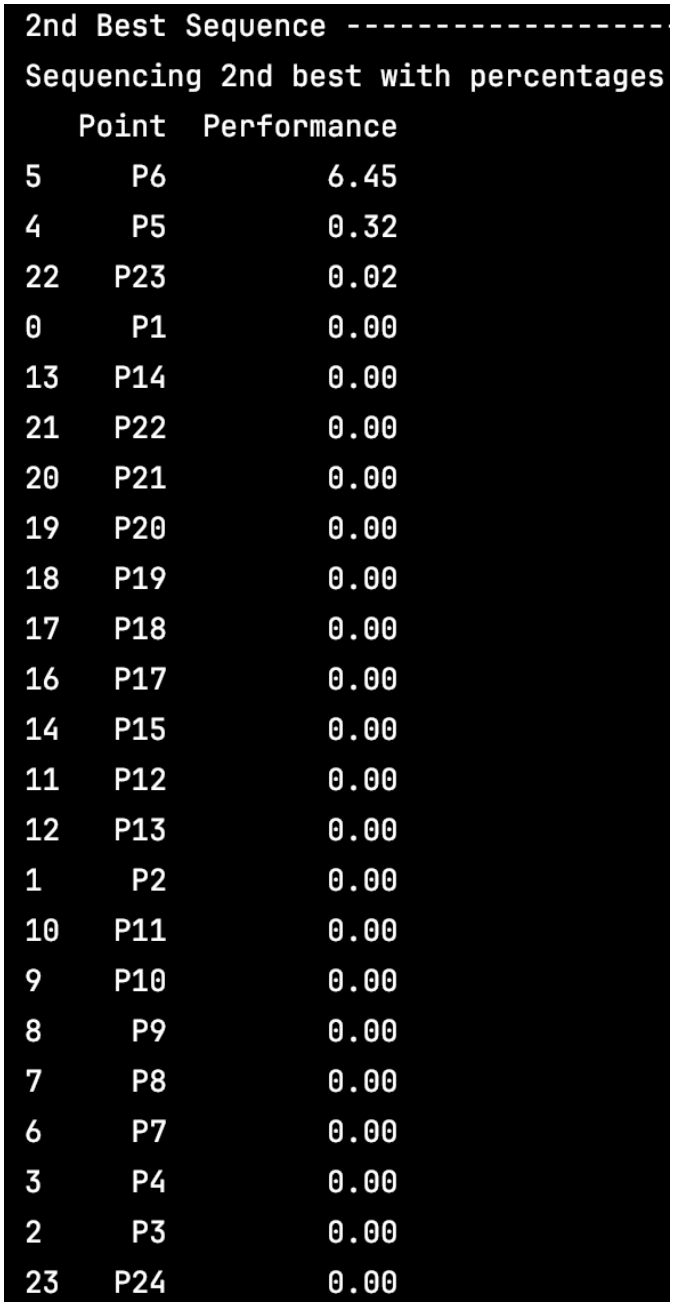


Figure 10. Sequencing's Second Next Best Point Selection With Performance Percentages.

List Unstable Row Sets

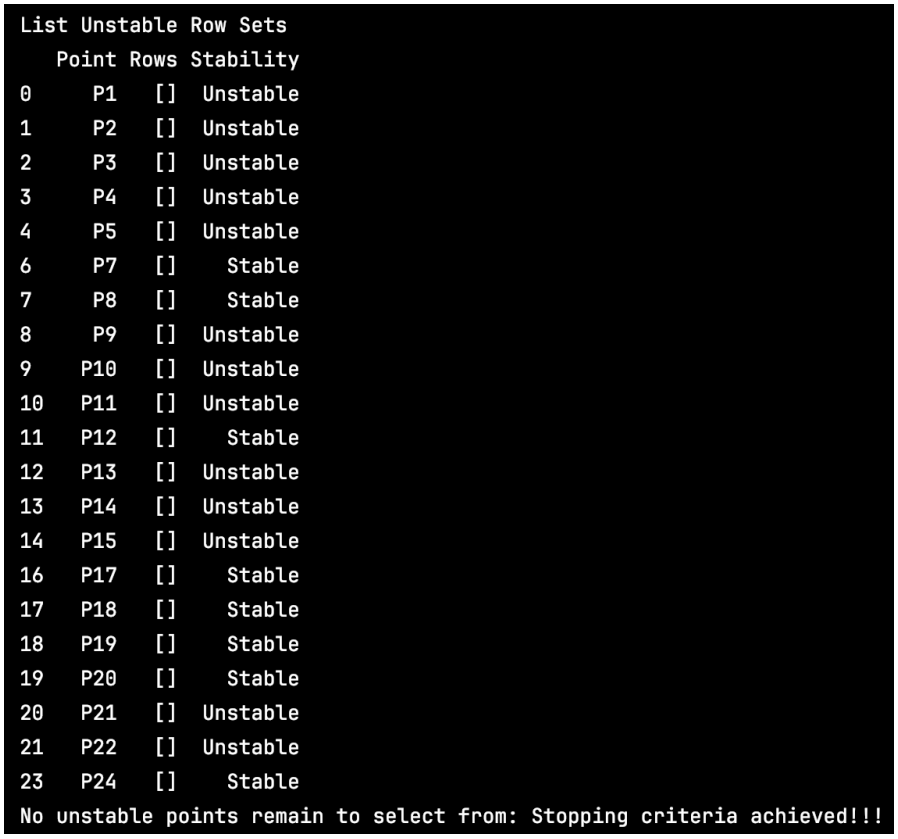
	Point	Rows	Stability
0	P1	[]	Unstable
1	P2	[]	Unstable
2	P3	[]	Unstable
3	P4	[]	Unstable
4	P5	[]	Unstable
6	P7	[]	Stable
7	P8	[]	Stable
8	P9	[]	Unstable
9	P10	[]	Unstable
10	P11	[]	Unstable
11	P12	[]	Stable
12	P13	[]	Unstable
13	P14	[]	Unstable
14	P15	[]	Unstable
16	P17	[]	Stable
17	P18	[]	Stable
18	P19	[]	Stable
19	P20	[]	Stable
20	P21	[]	Unstable
21	P22	[]	Unstable
22	P23	[5410, 3797]	Unstable
23	P24	[]	Stable

Figure 11. List of Unstable Row Sets Remaining Used for Determining Sequencing's Third Next Best Point.

```
3rd Best Sequence ------------------

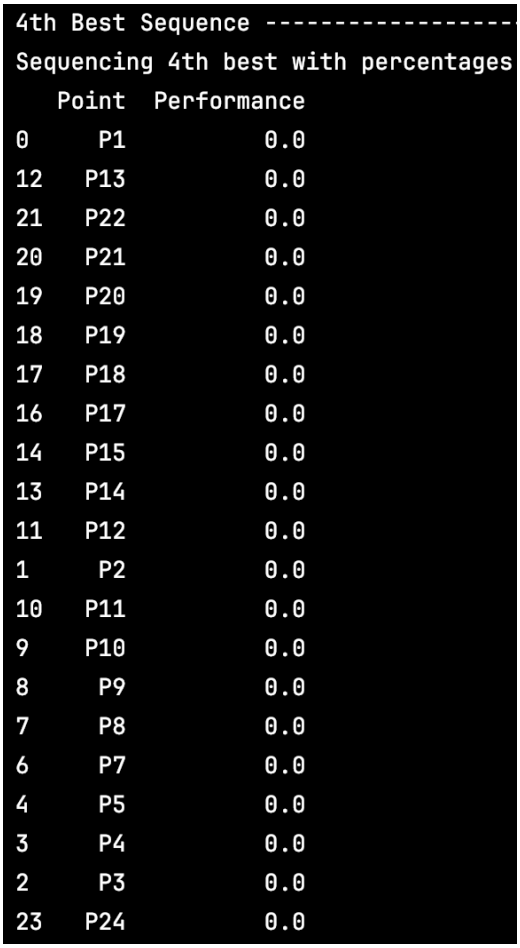
Sequencing 3rd best with percentages
   Point  Performance
22   P23         0.02
0     P1         0.00
1     P2         0.00
21   P22         0.00
20   P21         0.00
19   P20         0.00
18   P19         0.00
17   P18         0.00
16   P17         0.00
14   P15         0.00
13   P14         0.00
12   P13         0.00
11   P12         0.00
10   P11         0.00
9    P10         0.00
8     P9         0.00
7     P8         0.00
6     P7         0.00
4     P5         0.00
3     P4         0.00
2     P3         0.00
23   P24         0.00
```

Figure 12. Sequencing's Third Next Best Point Selection With Performance Percentages.



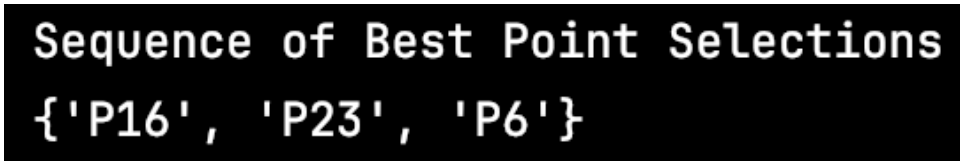
```
List Unstable Row Sets
   Point Rows Stability
0     P1   []  Unstable
1     P2   []  Unstable
2     P3   []  Unstable
3     P4   []  Unstable
4     P5   []  Unstable
6     P7   []    Stable
7     P8   []    Stable
8     P9   []  Unstable
9    P10   []  Unstable
10   P11   []  Unstable
11   P12   []    Stable
12   P13   []  Unstable
13   P14   []  Unstable
14   P15   []  Unstable
16   P17   []    Stable
17   P18   []    Stable
18   P19   []    Stable
19   P20   []    Stable
20   P21   []  Unstable
21   P22   []  Unstable
23   P24   []    Stable
No unstable points remain to select from: Stopping criteria achieved!!!
```

Figure 13. Empty List of Unstable Row Sets Remaining for Sequencing's Fourth Next Best Point & Displaying Stopping Criteria Reached.



```
4th Best Sequence ------------------
Sequencing 4th best with percentages
   Point  Performance
0     P1          0.0
12   P13          0.0
21   P22          0.0
20   P21          0.0
19   P20          0.0
18   P19          0.0
17   P18          0.0
16   P17          0.0
14   P15          0.0
13   P14          0.0
11   P12          0.0
1     P2          0.0
10   P11          0.0
9    P10          0.0
8     P9          0.0
7     P8          0.0
6     P7          0.0
4     P5          0.0
3     P4          0.0
2     P3          0.0
23   P24          0.0
```

Figure 14. Sequencing's Fourth Next Best Point Selection With Performance Percentages & Displaying Stopping Criteria Reached.

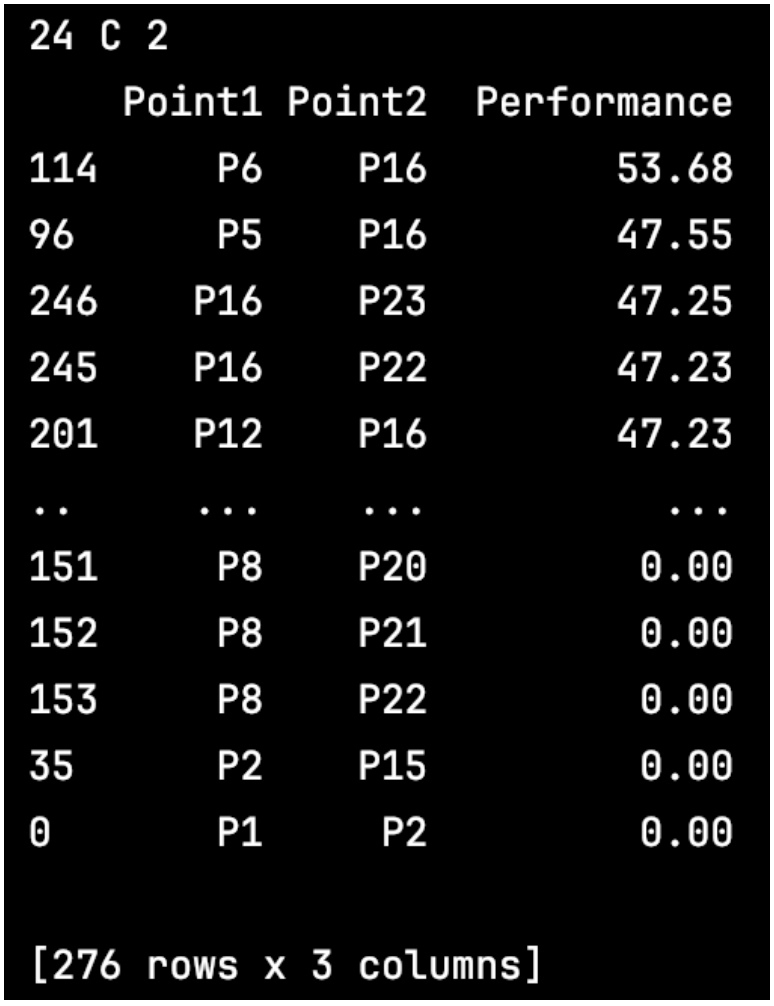


```
Sequence of Best Point Selections
{'P16', 'P23', 'P6'}
```

Figure 15. Sequence of Best Point Selections Based on Performance Percentages.

```
24 C 1
    Point  Performance
15    P16        47.23
5      P6        36.26
14    P15        13.82
4      P5        13.76
3      P4         8.69
13    P14         2.77
12    P13         0.35
2      P3         0.13
22    P23         0.02
21    P22         0.00
20    P21         0.00
19    P20         0.00
18    P19         0.00
17    P18         0.00
16    P17         0.00
0      P1         0.00
1      P2         0.00
11    P12         0.00
10    P11         0.00
9     P10         0.00
8      P9         0.00
7      P8         0.00
6      P7         0.00
23    P24         0.00
```

Figure 16. 24C1 Top Best Point Selection With Performance Percentages.



```
24 C 2
    Point1 Point2  Performance
114     P6    P16        53.68
96      P5    P16        47.55
246    P16    P23        47.25
245    P16    P22        47.23
201    P12    P16        47.23
..     ...    ...          ...
151     P8    P20         0.00
152     P8    P21         0.00
153     P8    P22         0.00
35      P2    P15         0.00
0       P1     P2         0.00

[276 rows x 3 columns]
```

Figure 17. 24C2 Best Points Selection With Performance Percentages.

```
24 C 3
     Point1 Point2 Point3  Performance
1178     P6    P16    P23        53.70
1063     P6     P7    P16        53.68
1121     P6    P11    P16        53.68
722      P4     P6    P16        53.68
1094     P6     P9    P16        53.68
...     ...    ...    ...          ...
1248     P7    P10    P20         0.00
1247     P7    P10    P19         0.00
1246     P7    P10    P18         0.00
1245     P7    P10    P17         0.00
0        P1     P2     P3         0.00

[2024 rows x 4 columns]
```

Figure 18. 24C3 Best Points Selection With Performance Percentages.

```
24 C 4
     Point1 Point2 Point3 Point4  Performance
2465     P2     P6    P16    P23         53.7
7498     P6    P16    P19    P23         53.7
7081     P6     P9    P16    P23         53.7
7452     P6    P15    P16    P23         53.7
925      P1     P6    P16    P23         53.7
...     ...    ...    ...    ...          ...
3977     P3     P8    P10    P12          0.0
3976     P3     P8    P10    P11          0.0
3975     P3     P8     P9    P24          0.0
3973     P3     P8     P9    P22          0.0
5313     P4     P9    P19    P22          0.0

[10626 rows x 5 columns]
```

Figure 19. 24C4 Best Points Selection With Performance Percentages.

```
24 C 5
      Point1 Point2 Point3 Point4 Point5  Performance
32619     P6    P10    P11    P16    P23         53.7
31306     P6     P7    P12    P16    P23         53.7
11448     P2     P5     P6    P16    P23         53.7
33291     P6    P12    P14    P16    P23         53.7
18900     P3     P6    P13    P16    P23         53.7
...      ...    ...    ...    ...    ...          ...
13995     P2     P8    P11    P12    P22          0.0
13994     P2     P8    P11    P12    P21          0.0
13993     P2     P8    P11    P12    P20          0.0
13992     P2     P8    P11    P12    P19          0.0
8548      P1    P14    P15    P19    P22          0.0

[42504 rows x 6 columns]
```

Figure 20. 24C5 Best Points Selection With Performance Percentages.

```
24 C 6
       Point1 Point2 Point3 Point4 Point5 Point6  Performance
33943      P2     P3     P4     P6    P16    P23         53.7
71647      P3     P6    P16    P17    P19    P23         53.7
24757      P1     P6    P14    P15    P16    P23         53.7
49201      P2     P6     P8    P10    P16    P23         53.7
113836     P6    P10    P15    P16    P19    P23         53.7
...       ...    ...    ...    ...    ...    ...          ...
27988      P1     P8    P10    P11    P21    P22          0.0
27987      P1     P8    P10    P11    P20    P24          0.0
87518      P4     P7     P8    P11    P17    P22          0.0
27985      P1     P8    P10    P11    P20    P22          0.0
28284      P1     P8    P11    P12    P13    P18          0.0

[134596 rows x 7 columns]
```

Figure 21. 24C6 Best Points Selection With Performance Percentages.

Point	RPM	Depth of cut (mm)	Width of cut (mm)	Feed Rate (mm/min)	MRR (cc/min)	MRR (cc/sec)	Cost of Point Test per sec ($)	Teeth #
4	6600	1	5	2640	13.2	0.22	$3.26	4
8	7400	1	5	2960	14.8	0.25	$3.65	**Feed per tooth mm/tooth**
12	8200	1	5	3280	16.4	0.27	$4.05	0.1
16	9000	1	5	3600	18	0.30	$4.44	**Cost per cc Removed ($)**
20	9800	1	5	3920	19.6	0.33	$4.84	14.8018648
24	10600	1	5	4240	21.2	0.35	$5.23	**Cost of 6061-T6 Aluminum Workpiece Block ($)**
3	6600	2	5	2640	26.4	0.44	$6.51	154.44
7	7400	2	5	2960	29.6	0.49	$7.30	**Length (mm)**
11	8200	2	5	3280	32.8	0.55	$8.09	1828.8
15	9000	2	5	3600	36	0.60	$8.88	**Width (mm)**
19	9800	2	5	3920	39.2	0.65	$9.67	25
2	6600	3	5	2640	39.6	0.66	$9.77	**Height (mm)**
23	10600	2	5	4240	42.4	0.71	$10.46	50
6	7400	3	5	2960	44.4	0.74	$10.95	**Block Volume (cc)**
10	8200	3	5	3280	49.2	0.82	$12.14	2286
1	6600	4	5	2640	52.8	0.88	$13.03	
14	9000	3	5	3600	54	0.90	$13.32	
18	9800	3	5	3920	58.8	0.98	$14.51	
5	7400	4	5	2960	59.2	0.99	$14.60	
22	10600	3	5	4240	63.6	1.06	$15.69	**Note:**
9	8200	4	5	3280	65.6	1.09	$16.18	https://www.mcmaster.com/products/bars/multipurpose-6061-aluminum-sheets-and-bars-7/shape-type~bar-1/
13	9000	4	5	3600	72	1.20	$17.76	
17	9800	4	5	3920	78.4	1.31	$19.34	
21	10600	4	5	4240	84.8	1.41	$20.92	

Figure 22. Excel Spreadsheet Showing Each Point's MRR and Cost Per Test.

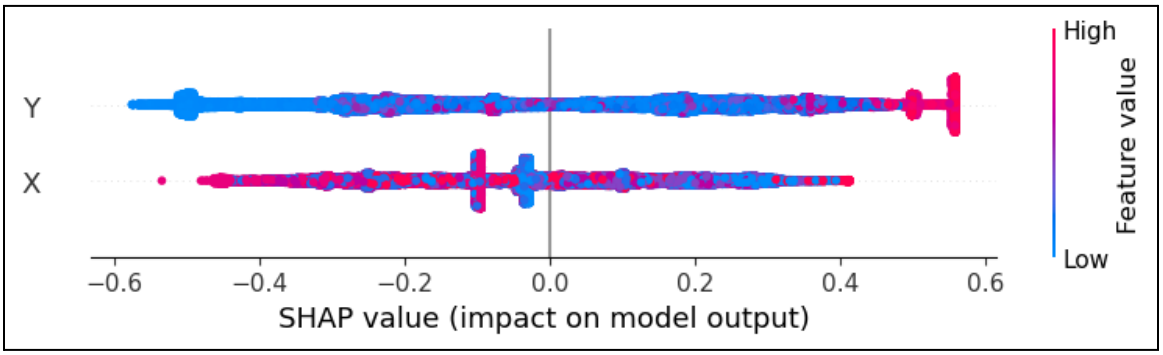


Figure 23. SHAP Analysis Summary Plot Output.

VITA

Kaitlyn C. Daniels was born in Knoxville, Tennessee, on September 6, 2000. She attended and graduated as Valedictorian from the Seymour High School in the Sevier County School system in May 2019. The following school year, she entered the University of Tennessee where she graduated in May 2023 with her Bachelor's Degree in Industrial Engineering with a double minor in Leadership and Reliability and Maintainability (RME). She then proceeded to work as a Graduate Teaching Assistant and then a Graduate Research Apprentice while pursuing her education. She is in the process of completing her Master's Degree in Industrial Engineering where she wrote this thesis. She is also working to earn her Fire Protection Engineering Certification by the end of the summer of 2024. She plans to continue her education at the University of Tennessee in August 2024 by pursuing a PhD in Biosystems Engineering with ambitions of becoming a professor.